

Identification of a Model Agnostic Disease Driver in  
Non-alcoholic Steatohepatitis; Implications for Drug  
Development

Kimberly Liao

## Abstract

Currently, there is a strong prevalence of non-alcoholic steatohepatitis (NASH), affecting a third of all American adults. This asymptomatic disease is closely associated with obesity and diabetes. NASH, which begins as non-alcoholic fatty liver disease (NAFLD), can further progress to NASH with increasing levels of fibrosis, cirrhosis and even hepatocellular carcinoma (HCC). Currently, there is no approved therapy for NASH and a number of therapeutics that has met success in the laboratory has fared poorly in clinical trials. Therefore, this study suggests a model agnostic approach to identify a disease driver in mice models that also corresponds to human NASH. Adult mice were separated by three treatments: fast food diet (FFD), FFD + thioacetamide, and FFD + CCl<sub>4</sub> + glucose water; the 3 produced models each represent a stage of the NAFLD progression. Histopathological features were semi-quantitated on the basis of NAFLD activity score (NAS) and for fibrosis severity. Transcriptomic analysis was conducted through quantitative polymerase chain reaction (qPCR), and based on mRNA data, the majority experienced increased expression in the models representing NASH with fibrosis. However, the *gpat1* gene to be sustained across all three models studied. The early detection and continued expression of *gpat1* and its strong correlation with NAS suggests the functional significance of this disease driver in human NASH.

## Identification of a Model Agnostic Disease Driver in Non-alcoholic Steatohepatitis: Implications for Drug Development

### Background

With the recent rise in diabetes, obesity, and metabolic syndrome, non-alcoholic fatty liver disease (NAFLD) has reached epidemic proportions; one in three Americans are diagnosed with the disease [1-2]. Currently, a stage of NAFLD – non-alcoholic steatohepatitis (NASH) – has even greater implications. NASH, characterized by steatosis and inflammation, is predicted to become the primary cause for liver transplants in the next five years [4]. NASH is often called a “silent” disease as most patients experience no symptoms [2]. The complications associated with this asymptomatic disease lie in its progression to NASH with fibrosis, which could further develop into cirrhosis and possibly hepatocellular carcinoma (HCC) if untreated [3-5]. However, evidence [5] suggests that NASH can also progress to HCC prior to cirrhosis (Figure 1), indicating the NASH stage as a pivotal point in the NAFLD progression.

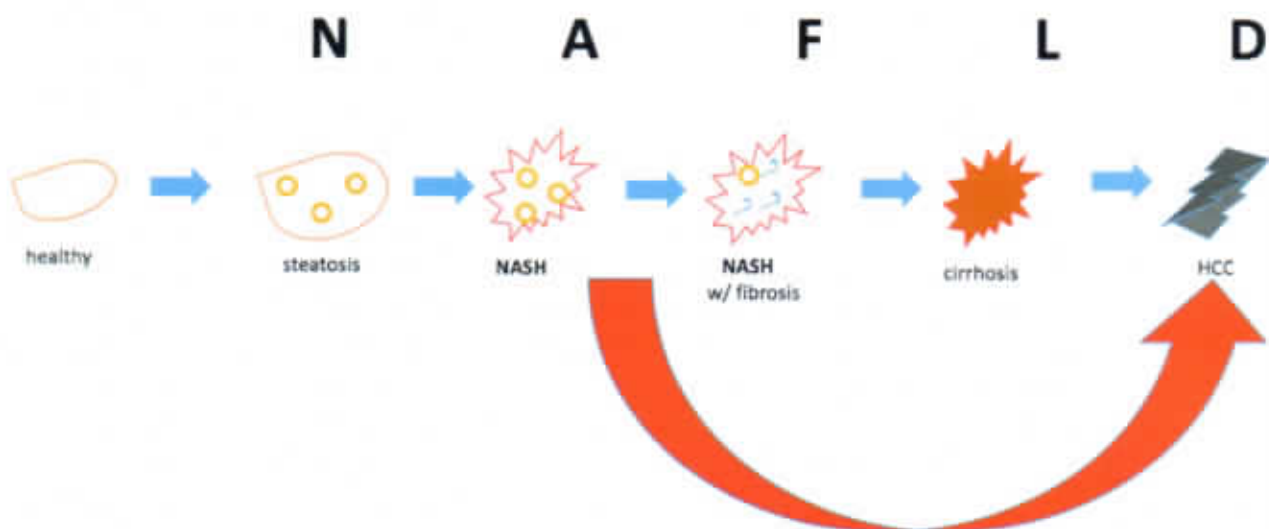


**Fig 1. NAFLD Continuum.** Accumulation of fat in the liver (steatosis stage) can lead to NASH and further progress to NASH with fibrosis – scarring of the liver. Furthermore, cirrhosis, significant scarring of the entire liver, may follow, enhancing risk for HCC. However, during the NASH stage, HCC can also occur in absence of cirrhosis (red arrow) [5].

Unlike other organ-targeted diseases wherein function can be managed mechanically (e.g. dialysis in patients with kidney disease), a new liver, which is hard to come by, remains the mainstay for management of end-stage kidney disease. To date, no drug has proven sufficiently effective in reversing or even halting liver inflammation and scarring [3]. There are also no

approved therapies for NASH with fibrosis to date [6]. In part, the lack of treatments can be accredited to the clinical punctuated with failures (Selonsertib/Gilead and emricansan/Conatus-Novartis) [7-8], marginal success accompanied by significant side effects (Ocaliva/Intercept) [9] or merely limited success (PIVENS and REGENERATE) [10-11]. The weak translational data can be explained by the inherent disconnect between animal models wherein the drug is evaluated and human liver disease where the drug is expected to work and the inconsistency exhibited in how biochemical/histopathological endpoints are governed in each unique patient [2, 6].

There is currently a fundamental shift from studies focused on the function of single molecules or single pathways in a model system to bench-to-bedside-enabling research. The shift is employed using information-rich multi-dimensional data sets drawn from the generation of hypotheses [6,12]. The looming challenge for biomedical sciences is to decipher biological knowledge from high-dimensional data – biological function of individual genes, pathways, and networks that drive complex phenotypes – and translate that to tangible outcomes [13]. This can be achieved through the integration of a diversity of data such as through integrative systems biology [14]. Systems biology combines complex biological information and has the power to provide a comprehensive description of regulatory events in NASH with fibrosis.

It is abundantly clear that NASH is an area of tremendous unmet medical need and given the sheer size of this burgeoning epidemic, a treatment strategy is urgently required that can prevent its transition to scarring and the sequelae of scarring.

## **Hypothesis**

The observed failure of clinical trials in NASH and lack of robust translational success suggest that the current model systems do not fully recapitulate human disease and the hallmark pathological features of NASH may not be caused by the same pathway in animal models and human subjects. Therefore, it is hypothesized that model agnostic (model independent) disease driver is likely to play a role in human NASH. Identification of such disease-driver can spur development of drugs that neutralizes the driver and bridges the disconnect between animal models and human subjects.



## Approach

To employ disruptive and potentially highly impactful approach termed model agnostic functional transcriptomic analysis to identify a disease driver in NASH (Figure 2).

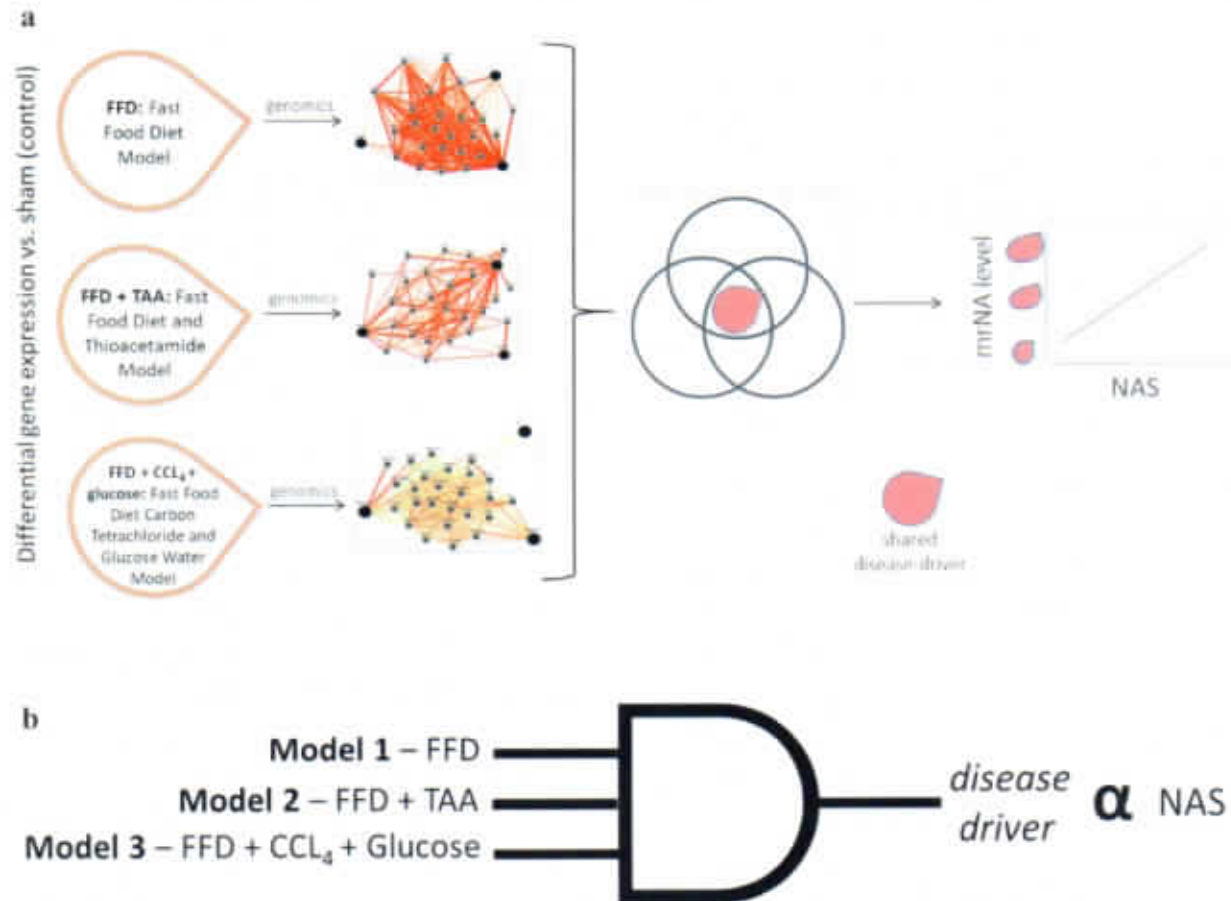


**Figure 2. Functional Transcriptomic Mapping.** **a)** A gene ontology-driven search was conducted to identify and query a set of genes (mRNA/qPCR) across 3 distinct models of NASH. Transcriptomic data from the 3 models were overlapped (Venn diagram) to identify one or more common genes. Gene expression level was then correlated against NAFLD Activity Score (NAS, blinded observer) to confirm gene function. If the expression of the identified gene was increased across all 3 models and titrated NAS, it was deemed a functional disease driver and submitted as a target of interest for drug development. **b)** Boolean expression of the above.

## Methods

Banked hematoxylin-eosin-stained (H&E) and picrosirius red-stained (PSR) liver slides from 3 distinct murine models of NASH were utilized in this study. Banked frozen liver homogenates of these models were also utilized for RNA isolation, cDNA synthesis, and quantitative real-time polymerase chain reaction (qPCR) (IACUC #2019-014). All animals (n =

4 per cohort) had been previously sacrificed and liver samples had been previously collected for histopathological (10% formalin) or transcriptomic (liquid N<sub>2</sub>) analysis for an unrelated study.

### *I. Animal Models:*

**Sham (control) cohort:** Adult male C57BL/6 mice (18-20 g) had been randomized to standard rodent diet (sham) for 12 weeks. Drinking water was provided *ad libitum*.

**Model 1 – FFD cohort:** Adult male C57BL/6 mice (18-20 g) had been randomized to standard rodent diet (sham) or a fast food diet (FFD - rodent diet with 40 kcal% fat, 20 kcal% fructose and 2% cholesterol; D09100301, Research Diets, NJ) for 12 weeks [15-16]. Drinking water was provided *ad libitum*.

**Model 2 – FFD + TAA cohort:** Adult male C57BL/6 mice (18-20 g) had been randomized to standard rodent diet (sham) or a fast food diet (FFD - rodent diet with 40 kcal% fat, 20 kcal% fructose and 2% cholesterol; D09100301, Research Diets, NJ) for 12 weeks. Drinking water was provided *ad libitum*. Additionally, the FFD cohort was administered thioacetamide (TAA, 100 mg/kg, IP X 3/week; TAA is a liver scarring agent) for 12 weeks [17]. Drinking water was provided *ad libitum*.

**Model 3 – FFD + CCL<sub>4</sub> + glucose:** Adult male C57BL/6 mice (18-20 g) had been randomized to standard rodent diet (sham) or a fast food diet (FFD - rodent diet with 40 kcal% fat, 20 kcal% fructose and 2% cholesterol; D09100301, Research Diets, NJ) for 12 weeks. Drinking water was provided *ad libitum*. Additionally, the FFD cohort was administered carbon tetrachloride (CCL<sub>4</sub>) (0.32 µg/g, IP x 1/week; CCL<sub>4</sub> is a liver scarring agent) +18.9 g/L d-glucose in the drinking water for 12 weeks [15].

### *II. Liver histopathology (NAS and fibrosis)*

Histopathological analysis was utilized to verify presence of disease and for semi-quantitation. Hematoxylin-eosin (H&E)-stained liver sections were studied under a microscope (blinded to group) and scored on basis of the NAFLD Activity Score (NAS). The scoring system on 0–8 scale (8 being most diseased) totals the individual component scores for steatosis (0–3), lobular inflammation (0–3), and hepatocyte ballooning (0–3) [5, 18-19]. Picrosirius red (PSR) staining of liver sections were semi-quantified for extracellular fibrillar collagen using Bioquant

Image Analysis [20]. Quadruplicates for liver slide were scored for NAS and fibrosis to ensure the quantitation encompassed the whole liver.

### *III. Transcriptomic Analysis*

A literature-based gene campaign was first conducted to identify candidate genes of interest in NASH (Table 1) [21-23]. The level of gene expression in all liver tissue samples were measured by two-step quantitative polymerase chain reaction (qPCR) [24-25]. The Qiagen RNeasy Mini Kit was used to extract total RNA from sham (control) and toxin-induced NASH (experimental) liver samples according to manufacturer's instructions and stored at -80°C. cDNA was then synthesized from the extracted RNA using the Thermofisher High-Capacity cDNA Reverse Transcription Kit and a BioRad S1000 Thermocycler following manufacturer protocol. Samples were diluted 1:5 with nuclease free H<sub>2</sub>O, and stored at -20°C for qPCR, and the threefold diluted products were used for quantitative real-time PCR (qPCR). SYBR-Green qPCR was performed with Thermofisher Power-Up SYBR Green Master-Mix and using gene-specific forward and reverse primers were generated based on sequencing data from NCBI and designed using Primer3Plus primer-design tools. Designed primer sequences (Table 1) were produced using Oligo Sigma services (Millipore-Sigma; Massachusetts, U.S). qPCR was performed on a Thermofisher Quant-Studio 3 Real-Time PCR system; each qPCR reaction was performed in triplicate for all tissue samples following Power-Up SYBR Green manufacturer protocol for Fast qPCR for a total volume of 10 µl.



**Table 1. Targeted Genes and Respective Primers.** Twelve genes reported to experience up-regulation in models of NASH were identified. Genomic sequences of designed forward and reverse primers are exhibited.

Gene	Forward Primer Sequence	Reverse Primer Sequence
<i>Coll</i>	TCAGCTGCATACACAATGGC	ATTGCATTGCACGTCATCGC
<i>Gpat1</i>	CAATGAAACGCACACAAGGC	AACACTGGTGGCAAACATGC
<i><math>\alpha</math>SMA</i>	TACAGGTTTGCCTGACATG	TGTTCTCACGATGCCAATGC
<i>MMP2</i>	TGGCAGTGCTTTTCTCTGC	TCTTGCGGTTTCTCTTGCC
<i>IL1<math>\beta</math></i>	ATGAAGGGCTGCTTCCAAAC	ATGTGCTGCTGCGAGATTG
<i>CCL2</i>	ATTTTCCAGTGCCCCTTTGG	AACACGCATGAGCTGTTTCTAG
<i>IL6</i>	ACAAAGCCAGAGTCCTTCAGAG	TGGAAATTGGGGTAGGAAGGAC
<i>ICAM1</i>	TCAAAACCGAGAGCACAGTG	TTTCTGCCATCAGCTGTCTG
<i>CTGF</i>	TTCAGCAATGGCCTCGATTG	AATCGCGAGTGTGAGCAAAG
<i>TIMP1</i>	TCGTAGCAAACCACCAAGTG	TTTGAGATCCATGCCGTTGG
<i>TNF<math>\alpha</math></i>	TGGTGTGCTGTTGTCCTTG	TGGTGTCAAGCAACCAAGTG
<i>PPAR<math>\alpha</math></i>	TCCCAGGCTTTGCAAACCTTG	ATAAAGCCATTGCCGTACGC

#### IV. Data Analysis

All data (NAS, scarring, mRNA) was recorded and organized on Microsoft Excel. NAS data were presented as mean scores in each group. Liver scarring (PSR) data were presented as fold-change in relation to the sham cohort. mRNA levels were presented as fold-change in relation to the sham cohort as well. A student's T-test (p-value) was used to compare data diseased cohorts to sham cohort. Microsoft Excel was used for the NAS vs. mRNA correlation and to calculate Pearson product moment ( $r$ ) and the p-value.



## Results

After analysis of the liver histopathology through the use of NAS and fibrosis semi-quantitation, the presence of NASH disease was verified through exhibition of steatosis, lobular inflammation, and hepatocyte ballooning in the H&E-stained slides (Figure 3a). NASH with fibrosis was verified through the presence of bridging fibrosis in PSR-stained slides (Figure 3b).

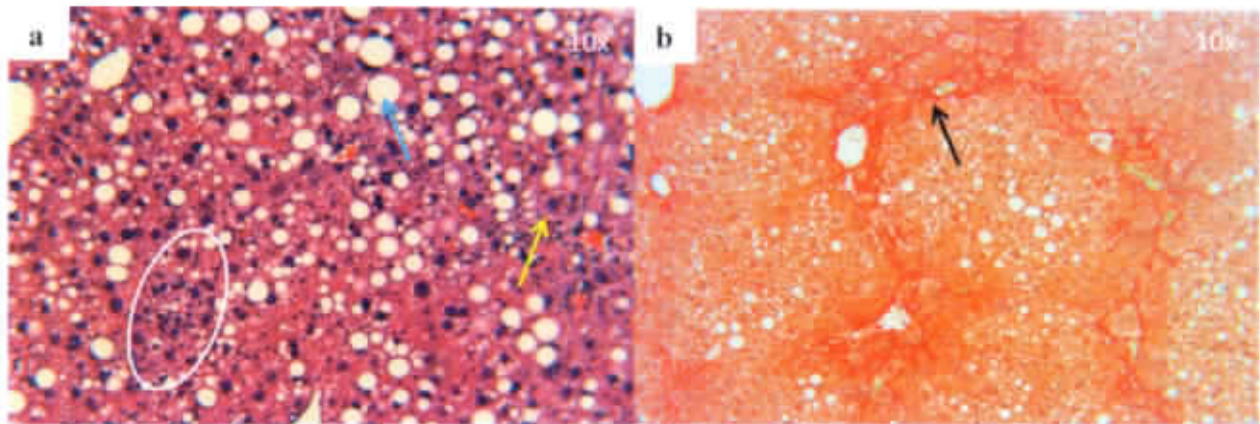


**Figure 3. NAS and Fibrosis.** **a)** H&E-stained slide of FFD + CCL<sub>4</sub> + glucose cohort. Steatosis (blue arrow) is characterized by lipid deposition. Lobular inflammation (white circle) refers to a linear cluster of inflamed cells. Hepatocyte ballooning (yellow) denotes a darker, cloudy cell with a prominent nucleus. **b)** PSR-stained slide of FFD + CCL<sub>4</sub> + glucose cohort. Bridging fibrosis across lobules (black arrow) is exhibited.

In consideration of the livers on modified diets presented with increased NAS (when comparing NAS,  $p < 0.01$  vs. sham), only model 2 (FFD + TAA) and model 3 (FFD + CCL<sub>4</sub> + glucose) exhibited scarring (PSR,  $p < 0.01$  vs. sham). Model 1, however, showed the greatest presences of lipid deposition.

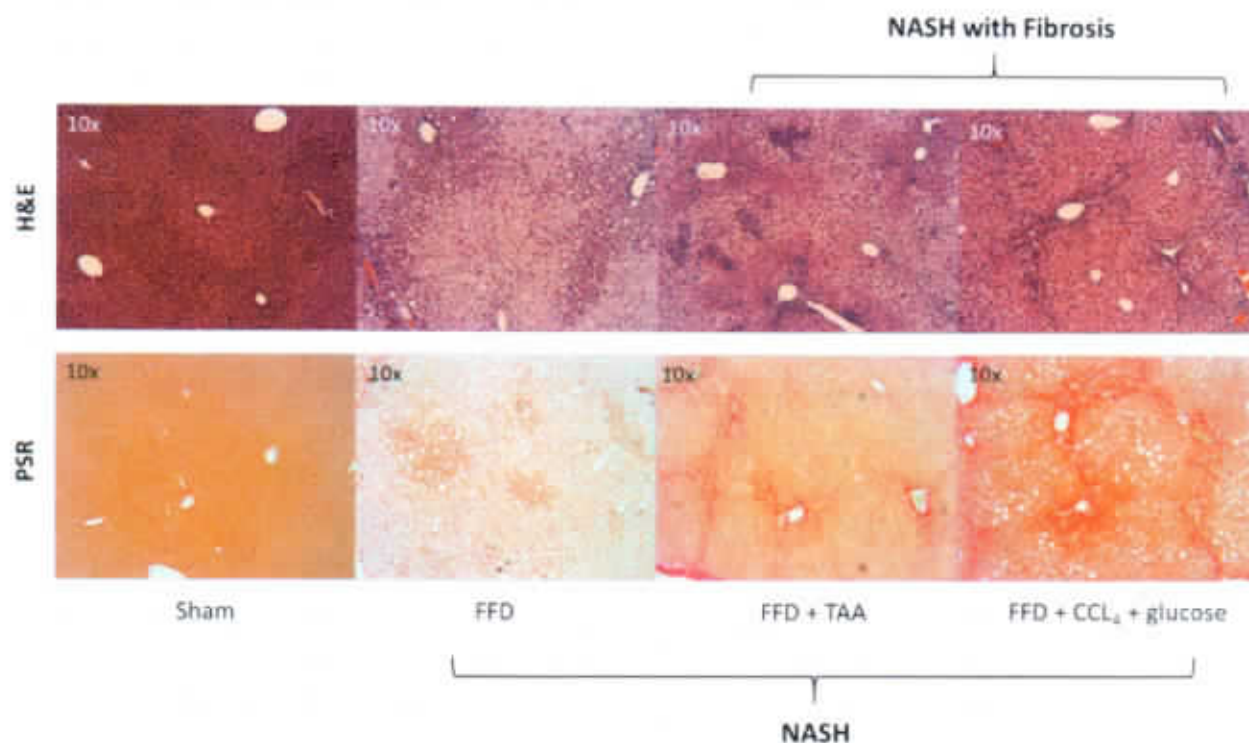


**Figure 4. Histopathological Overview of all four models.** Livers from animals on modified diet exhibited increased steatosis, inflammation and ballooning compared to animals on standard diet (sham). Only the FFD + TAA and FFD + CCl<sub>4</sub> + glucose water cohorts (not FFD alone) exhibited bridging fibrosis at this stage, classifying these models as diseased of NASH with fibrosis.

Table 2 reports the semi-quantitated histopathological features: NAFLD activity score (NAS) on H&E stained slides and fibrosis severity on PSR stained slides.

**Table 2. Semi-quantitative Histopathology. Animals on modified diet exhibited increased NAS compared to animals on standard diet (sham).** Only the FFD + TAA and FFD + CCl<sub>4</sub> + Glucose cohorts exhibited increased scarring (PSR, fold-increase in relation to sham), \*,  $p < 0.01$  vs. sham, blinded observer.

Model	NAS (H&E)	Fibrosis (PSR)
Sham	0	1
FFD	5*	0.97
FFD + TAA	5*	7.90*
FFD + CCl <sub>4</sub> + Glucose	5*	8.00*

In reference to mRNA data produced from qPCR trials, of all the genes queried (Table 3), *gpat1* was identified as the only node perturbed across all 3 models. *Gpat1* was upregulated early in liver disease (FFD – NASH without scarring); its upregulation was sustained in liver disease (FFD + TAA and FFD + CCl<sub>4</sub> + Glucose – NASH with scarring). Other genes were either modified late in disease (NASH with scarring) or not modified across all 3 models evaluated.

**Table 3. Transcriptomic Analysis.** Overview of transcriptomic results expressed as fold-increase in relation to sham. For most targeted genes, expression remained unchanged which is denoted as 1 in more than one model. *Gpat1* exhibited a sustained increased expression across all three models. \*, p<0.01 vs. sham.

Model	<i>COL1</i>	<i>GPAT1</i>	<i>αSMA</i>	<i>MMP2</i>	<i>IL1β</i>	<i>CCL2</i>	<i>IL6</i>	<i>ICAM1</i>	<i>CTGF</i>	<i>TIMP1</i>	<i>TNFα</i>	<i>PPARα</i>
Sham (control)	1	1	1	1	1	1	1	1	1	1	1	1
FFD (model 1)	1	5*	1	1	1	1	7*	1	1	1	1	1
FFD +TAA (model 2)	30*	4.9*	1	10*	2.2*	14*	1	2*	1	1	8*	1
FFD + TAA + Glucose (model 3)	8*	5.7*	1	8*	2.4*	1	1	1	1	10*	3*	1

Expression of some genes (*αSMA* and *ppara*) remained unchanged. *Ppara* was not perturbed in these models, and may in part explain the limited success of the PIVENS trial [10]. Additionally, the expression of other genes increased in some of the models, but not all. These expressions were most often present in NASH with fibrosis models (model 2 and model 3), indicating expression only during the latter stages of NASH. Although informative, expression in the fibrosis stage does not aid in early detection. Only *gpat1* expression exhibited a sustained increased across all 3 models.

Furthermore, *gpat1* expression level correlated directly with NAS (Figure 5) suggesting that this disease driver is of functional significance in NASH.

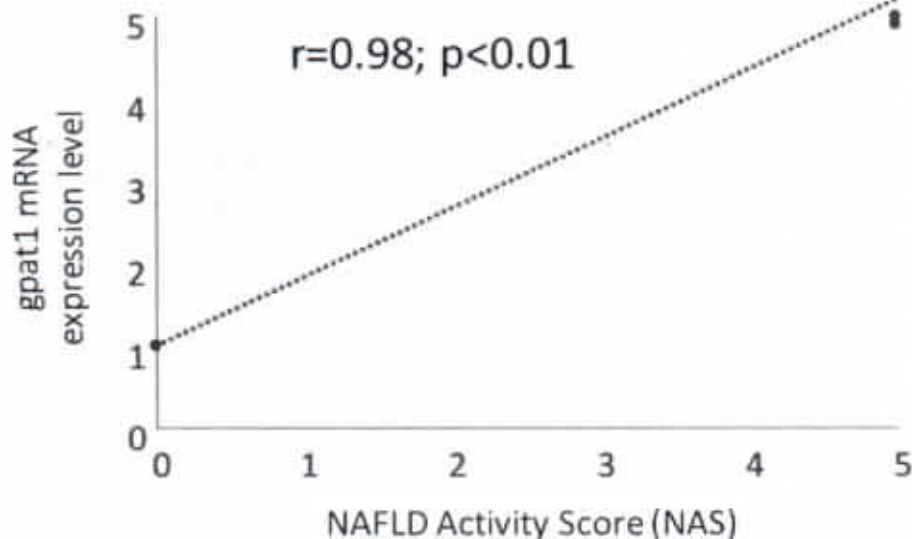


**Figure 5. Functional Transcriptomic Analysis.** *gpat1* mRNA expression level as a fold-increase in relation to sham correlated with NAS (data from Table 2 and 3). Exhibited a direct and highly significant correlation with NAS.

## Discussion

A multi-model functional transcriptomic analysis suggests that *gpat1* is a disease driver in NASH. Expression of *gpat1* was model agnostic, began in the earliest stage and was sustained, and correlated directly with NAS.

Approximately 30% of adults in the United States have some fat deposition (steatosis) in their livers, and 3–12% of adults in the United States are diagnosed with NASH [2–4]. Equally worrisome, given that a subset of NASH transitions directly to HCC, it is anticipated that fatty-liver related HCC will overtake all other causes of primary liver cancer with the next 2 or 3 decades [3]. Given the sheer size of these statistics there is an urgent need to develop therapeutics that prevent or at least restrain the NAFLD continuum. Presently, NASH therapeutics have fared poorly in clinical trials, and there is a dire need for a successful treatment to serve the needs of the growing NASH-inflicted population [6–11].

The overarching hypothesis driving this study was that a model agnostic disease driver is likely to play a role in human NASH. Identification of a pathway that is relevant in multiple



models of disease has a greater likelihood of being relevant in human disease. Furthermore, identification of such a disease-driver can spur development of drugs that neutralize that driver not only in animal models but also in human subjects. To this end, I queried samples from 3 etiologically different models of NASH. Although each model had the common clinically relevant thread of fast food diet, two of the models used additional additives to simulate oxidant stress and inflammation to accelerate disease. In fact, all 3 models exhibited hallmark pathological features of NASH (steatosis, lobular inflammation, hepatocyte ballooning) with two of the models also accompanied by scarring (fibrosis). Following state-of-the-art transcriptomic analysis conducted in liver homogenates, *gpai1* emerged as the only common denominator (in the set of genes queried) across all 3 models. While expression of some of the other genes such as *coll* was elevated only late in disease (NASH with fibrosis models), *gpai1* elevation was early-detected and continuous. Its expression exhibited a strong correlation with NAS, indicating the gene's role as a disease-driver.

GPAT1 is an enzyme that resides in hepatocytes, amongst other cells, and is involved in triacylglycerol accumulation [26]. In fact, an absence of GPAT1 protected mice from high fat diet-induced and genetic-induced hepatic steatosis [27]. This finding together with the findings reported above provide support for *gpai1* as a key player in the NAFLD continuum and suggest that development of agents that neutralize this target might prove efficacious in human NASH.

The implication of these findings should not be underestimated. These findings have triggered a campaign with Angion Biomedica to develop novel orally bioavailable drugs that neutralize GPAT1. If preclinical proof-of-concept studies with such a drug are successful it will trigger safety and efficacy studies with a GPAT1 inhibitor in biopsy-proven NASH patients overexpressing this disease-driver. Finally, as is occurring in oncology [28], a GPAT1 inhibitor would find use in tissue/disease agnostic basket trials involving subsets of patients whose disease (lung, kidney etc.) is being driven by *gpai1*. Results from this study have the potential to leverage the platform of Precision Medicine for a number of indications.

## References

1. Oscini, A. M., & Sanyal, A. J. (2017). Therapies in non-alcoholic steatohepatitis (NASH). *Liver international : official journal of the International Association for the Study of the Liver*, 37 Suppl 1(Suppl 1), 97–103. doi:10.1111/liv.13302.
2. Tesfay, M., Goldkamp, W. J., & Neuschwander-Tetri, B. A. (2018). NASH: The Emerging Most Common Form of Chronic Liver Disease. *Missouri medicine*, 115(3), 225–229.
3. Sanyal, A. J., Friedman, S. L., McCullough, A. J., Dimick-Santos, L., American Association for the Study of Liver Diseases, & United States Food and Drug Administration (2015). Challenges and opportunities in drug and biomarker development for nonalcoholic steatohepatitis: findings and recommendations from an American Association for the Study of Liver Diseases-U.S. Food and Drug Administration Joint Workshop. *Hepatology (Baltimore, Md.)*, 61(4), 1392–1405. doi:10.1002/hep.27678.
4. Charlton, M. R., Burns, J. M., Pedersen, R. A., Watt, K. D., Heimbach, J. K., Dierkhising, R. A. (2011). Frequency and outcomes of liver transplantation for nonalcoholic steatohepatitis in the United States. *Gastroenterology*, 141(4), 1249–53.
5. Hwang, A., Shi, C., Zhu, E., Naaz, F., Zhou, P., Rasheed, Z., ... Narayan, P. (2018). Supervised learning reveals circulating biomarker levels diagnostic of hepatocellular carcinoma in a clinically relevant model of non-alcoholic steatohepatitis; An OAD to NASH. *PloS one*, 13(6), e0198937. doi:10.1371/journal.pone.0198937.
6. Clarke, J. D., & Cherrington, N. J. (2015). Nonalcoholic steatohepatitis in precision medicine: Unraveling the factors that contribute to individual variability. *Pharmacology & therapeutics*, 151, 99–106. doi:10.1016/j.pharmthera.2015.03.005.
7. Gilead Announces Topline Data From Phase 3 STELLAR-4 Study of Selonsertib in Compensated Cirrhosis (F4) Due to Nonalcoholic Steatohepatitis (NASH) (2019). Retrieved on November 4, 2019, <https://www.gilead.com/news-and-press/press-room/press-releases/2019/2/gilead-announces-topline-data-from-phase-3-stellar4-study-of-selonsertib-in-compensated-cirrhosis-f4-due-to-nonalcoholic-steatohepatitis-nash>.
8. Emricasan fails to meet primary endpoint in NASH-cirrhosis trial (2019). Retrieved on November 4, 2019, <https://www.healio.com/hepatology/steatohepatitis-metabolic-liver-disease/news/online/%7B9cd2b213-a5b5-4a89-9b52-29f0a3501cad%7D/emricasan-fails-to-meet-primary-endpoint-in-nash-cirrhosis-trial>.
9. Intercept sputters as it reveals full Ocaliva NASH data to doctors (2019). Retrieved on November 4, 2019, <https://www.biopharmadive.com/news/intercept-sputters-as-it-reveals-full-ocaliva-nash-data-to-doctors/552549/>.
10. Sanyal, A., Chalasani, N., Kowdley, K., McCullough, A., Diehl, A., Bass, N... Robuck, P. (2010). Pioglitazone, Vitamin E, or Placebo for Nonalcoholic Steatohepatitis. *The New England Journal of Medicine*, 362(18): 1675–1685.
11. 'Watershed moment:' Ocaliva improves NASH in phase 3 trial (2019). Retrieved on November 10, 2019, <https://www.healio.com/hepatology/steatohepatitis-metabolic-liver-disease/news/online/%7B34a168a4-0b32-4daa-b0b6-0fa5a18772f7%7D/lqwatershed-momentrsquo-obeticholic-acid-improves-nash-in-phase-3-trial>.
12. What is precision medicine? (2015). <https://ghr.nlm.nih.gov/primer/precisionmedicine/definition>.
13. Vamathevan, J., Clark, D., Czodrowski, P., Dunham, I., Ferran, E., Lee, G., ... Zhao, S. (2019). Applications of machine learning in drug discovery and development. *Nature reviews. Drug discovery*, 18(6), 463–477. doi:10.1038/s41573-019-0024-5.



14. Dana, D., Gadhiya, S. V., St Surin, L. G., Li, D., Naaz, F., Ali, Q., ... Narayan, P. (2018). Deep Learning in Drug Discovery and Medicine; Scratching the Surface. *Molecules (Basel, Switzerland)*, 23(9), 2384. doi:10.3390/molecules23092384.
15. Tsuchida, T., Lee, Y. A., Fujiwara, N., Ybanez, M., Allen, B., Martins, S., ... Friedman, S. L. (2018). A simple diet- and chemical-induced murine NASH model with rapid progression of steatohepatitis, fibrosis and liver cancer. *Journal of hepatology*, 69(2), 385–395. doi:10.1016/j.jhep.2018.03.011.
16. Huang, B., Abbott, A. E., Dacon, L., McCormack, S., Zhou, P., Zhang, L., ... Narayan, P., Acute Injury in Natural Diet-Induced Fatty Livers - A Model for Therapy Development. *Recent Patents on Biomarkers*, 5(2), 1-7.
17. Sharma, L., Gupta, D., Abdullah, S. T., (2019). Thioacetamide potentiates high cholesterol and high fat diet induced steato-hepatic changes in livers of C57BL/6J mice: A novel eight weeks model of fibrosing NASH. *Toxicol Lett*, 304, 21-29. doi:10.1016/j.toxlet.2019.01.001.
18. Paka, L., Smith, D. E., Jung, D., McCormack, S., Zhou, P., Duan, B., ... Narayan, P. (2017). Anti-steatotic and anti-fibrotic effects of the KCa3.1 channel inhibitor, Senicapoc, in non-alcoholic liver disease. *World journal of gastroenterology*, 23(23), 4181–4190. doi:10.3748/wjg.v23.i23.4181.
19. Non-alcoholic Fatty Liver Disease (NAFLD) and Nonalcoholic Steatohepatitis (NASH) (2018). Retrieved on November 1, 2019, Non-alcoholic Fatty Liver Disease (NAFLD) and Nonalcoholic Steatohepatitis (NASH)
20. Hewitson, T. D., Smith, E. R., Samuel, C.S., (2014). Qualitative and quantitative analysis of fibrosis in the kidney. *Nephrology*, 19(11), 721–6.
21. Drescher, H. K., Weiskirchen, R., Fülöp, A., Hopf, C., de San Román, E. G., Huesgen, P. F., ... Kroy, D. C. (2019). The Influence of Different Fat Sources on Steatohepatitis and Fibrosis Development in the Western Diet Mouse Model of Non-alcoholic Steatohepatitis (NASH). *Frontiers in physiology*, 10, 770. doi:10.3389/fphys.2019.00770
22. Zhu, M., Li, M., Zhou, W., Yang, Y., Li, F., Zhang, L., & Ji, G. (2019). Qianggan extract improved nonalcoholic steatohepatitis by modulating lncRNA/circRNA immune ceRNA networks. *BMC complementary and alternative medicine*, 19(1), 156. doi:10.1186/s12906-019-2577-6
23. Lu, J., Li, J., Hu, Y., Guo, Z., Sun, D., Wang, P., ... Liu, P. (2019). Chrysophanol protects against doxorubicin-induced cardiotoxicity by suppressing cellular PARylation. *Acta pharmaceutica Sinica*, 40(4), 782–793. doi:10.1016/j.apsb.2018.10.008
24. Bethunaickan, R., Berthier, C. C., Zhang, W., Eksi, R., Li, H. D., Guan, Y., ... Davidson, A. (2014). Identification of stage-specific genes associated with lupus nephritis and response to remission induction in (NZB × NZW)F1 and NZM2410 mice. *Arthritis & rheumatology (Hoboken, N.J.)*, 66(8), 2246–2258. doi:10.1002/art.38679.
25. Berthier, C. C., Bethunaickan, R., Gonzalez-Rivera, T., Nair, V., Ramanujam, M., Zhang, W., ... Kretzler, M. (2012). Cross-species transcriptional network analysis defines shared inflammatory responses in murine and human lupus nephritis. *Journal of immunology*, 189(2), 988–1001. doi:10.4049/jimmunol.1103031.
26. Takeuchi, K., & Reue, K. (2009). Biochemistry, physiology, and genetics of GPAT, AGPAT, and lipin enzymes in triglyceride synthesis. *American journal of physiology. Endocrinology and metabolism*, 296(6), E1195–E1209. doi:10.1152/ajpendo.90958.2008
27. Wendel, A. A., Li, L. O., Li, Y., Cline, G. W., Shulman, G. I., & Coleman, R. A. (2010). Glycerol-3-phosphate acyltransferase 1 deficiency in ob/ob mice diminishes hepatic

steatosis but does not protect against insulin resistance or obesity. *Diabetes*, 59(6), 1321–1329. doi:10.2337/db09-1380

28. Chandanais, R., (2018). Basket Studies: An Innovative Approach for Oncology Trials, *Pharmacy Times*, Received on November 2, 2019, <https://www.pharmacytimes.com/contributor/ryan-chandanais-ms-cpht/2018/07/basket-studies-an-innovative-approach-for-oncology-trials>